

# Magnetic circular dichroism studies of the active site heme coordination sphere of exogenous ligand-free ferric cytochrome *c* peroxidase from yeast: effects of sample history and pH<sup>1</sup>

Alycen E. Pond<sup>a</sup>, Masanori Sono<sup>a</sup>, Elka A. Elenkova<sup>a,2</sup>, Duncan E. McRee<sup>b</sup>,  
David B. Goodin<sup>b</sup>, Ann M. English<sup>c</sup>, John H. Dawson<sup>a,d,\*</sup>

<sup>a</sup> Department of Chemistry and Biochemistry, University of South Carolina, Columbia, SC 29208, USA

<sup>b</sup> The Scripps Research Institute, La Jolla, CA 92037, USA

<sup>c</sup> Department of Chemistry and Biochemistry, Concordia University, Montreal H3G 1M8, Canada

<sup>d</sup> School of Medicine, University of South Carolina, Columbia, SC 29208, USA

Received 8 December 1998; received in revised form 2 July 1999; accepted 19 July 1999

## Abstract

Electronic absorption and magnetic circular dichroism (MCD) spectroscopic data at 4°C are reported for exogenous ligand-free ferric forms of cytochrome *c* peroxidase (CCP) in comparison with two other histidine-ligated heme proteins, horseradish peroxidase (HRP) and myoglobin (Mb). In particular, we have examined the ferric states of yeast wild-type CCP (YCCP), CCP(MKT) which is the form of the enzyme that is expressed in and purified from *E. coli*, and contains Met–Lys–Thr (MKT) at the N-terminus, CCP(MKT) in the presence of 60% glycerol, lyophilized YCCP, and alkaline CCP(MKT). The present study demonstrates that, while having similar electronic absorption spectra, the MCD spectra of ligand-free ferric YCCP and CCP(MKT) are somewhat varied from one another. Detailed spectral analyses reveal that the ferric form of YCCP, characterized by a long wavelength charge transfer (CT) band at 645 nm, exists in a predominantly penta-coordinate state with spectral features similar to those of native ferric HRP rather than ferric Mb (His/water hexa-coordinate). The electronic absorption spectrum of ferric CCP(MKT) is similar to those of the penta-coordinate states of ferric YCCP and ferric HRP including a CT band at 645 nm. However, its MCD spectrum shows a small trough at 583 nm that is absent in the analogous spectra of YCCP and HRP. Instead, this trough is similar to that seen for ferric myoglobin at about 585 nm, and is attributed (following spectral simulations) to a minor contribution ( $\leq 5\%$ ) in the spectrum of CCP(MKT) from a hexa-coordinate low-spin species in the form of a hydroxide-ligated heme. The MCD data indicate that the lyophilized sample of ferric YCCP ( $\lambda_{CT}=637$  nm) contains considerably increased amounts of hexa-coordinate low-spin species including both His/hydroxide and bis-His species. The crystal structure of a spectroscopically similar sample of CCP(MKT) ( $\lambda_{CT}=637$  nm) solved at 2.0 Å resolution is consistent with His/hydroxide coordination. Alkaline CCP (pH 9.7) is proposed to exist as a mixture of hexa-coordinate, predominantly low-spin complexes with distal His 52 and hydroxide acting as distal ligands based on MCD spectral comparisons. © 1999 Elsevier Science Inc. All rights reserved.

**Keywords:** Magnetic circular dichroism; Cytochrome *c* peroxidase; Horseradish peroxidase; Myoglobin; Cytochrome *b*<sub>5</sub>; Heme coordination sphere

## 1. Introduction

Cytochrome *c* peroxidase (CCP) is a soluble 34-kDa heme protein, located in the mitochondrial intermembrane space, that catalyzes the two-electron reduction of hydroperoxides (ROOH, R=H or alkyl) by ferrocycytochrome *c* [1]. The solution of the crystal structure of CCP [2,3] and the devel-

opment of cloning systems for the production of both wild-type and mutant forms of CCP [4,5] have enabled researchers to probe the heme active site more thoroughly. However, with increasing interest in the CCP system, some apparently conflicting observations have been reported on the effects of purification method, pH, handling, buffer and storage on the catalytic and spectroscopic properties of the enzyme.

The purification of CCP from yeast by the methods of Yonetani and Ray [6] produces enzyme with a purity index (PZ;  $A_{408}/A_{280}$ ) of 1.2 to 1.3. In contrast, more recent purification methods employing acetate buffers at acidic pH yield CCP with a PZ of about 1.5 [7,8]. However, resonance

\* Corresponding author. Tel.: +1-803-777-7234; fax: +1-803-777-9521; e-mail: dawson@psc.sc.edu

<sup>1</sup> The reviewing and handling of this manuscript was overseen by a member of the editorial board.

<sup>2</sup> Deceased.

Raman studies indicated that enzyme preparations with lower PZ values (1.25 to 1.3) have a five-coordinate high-spin heme [9] while CCP samples with a higher PZ of 1.5 are a mixture of five-coordinate and six-coordinate high-spin complexes [10]. This variation of coordination state homogeneity despite an increased PZ value indicates that the change in PZ value is due to differences in the absorption spectra of the various preparations. In fact, spectroscopic studies have led to the conclusion that native ferric CCP has two forms with differing coordination states, the distribution of which depends on the purification scheme, handling, and storage of the enzyme [9–11]. These two forms of CCP have been termed ‘fresh’ and ‘aged’. The ‘fresh’ form of CCP is the active form, and is in a predominantly penta-coordinate, high-spin state ( $S=5/2$ ), exhibiting a characteristic high-spin marker band at 645 nm and a high-spin EPR spectrum characteristic of rhombically distorted axial symmetry ( $g_{\perp}=6.4$ ,  $5.3$ ,  $g_{\parallel}=1.97$ ) [11]. Storage, exposure to acidic pH, or freezing of CCP results in the generation of the inactive ‘aged’ form of CCP [11]. The heme iron in this form of CCP is predominantly hexa-coordinate high-spin, having a high-spin marker band at a wavelength as low as 620 nm and an axially symmetric high-spin ( $S=5/2$ ) EPR spectrum ( $g_{\perp}=6$ ,  $g_{\parallel}=2$ ) [11]. Researchers concluded that changes in the protein conformation induced by storage and/or pH variation allow an internal weak field ligand (likely a distal solvent molecule) to coordinate axially to the heme iron. Therefore, the purity index, the location of the charge transfer (CT) band in the absorption spectrum (620 versus 645 nm) along with an ability or inability to react with hydrogen peroxide have all been used to determine the ‘freshness’ of CCP [9–11].

Recent studies by Vitello et al. [12] indicate that the ratio of absorptivity of the Soret maximum (408 nm) to that of the shoulder at 380 nm and the ratio of absorptivity at 620 nm relative to that of the CT band near 647 nm are more sensitive indicators of the presence of hexa-coordinate forms of CCP. Both of these ratios should increase with increasing amounts of hexa-coordinate protein. Using these ratios, Vitello and co-workers determined that storage of the protein at  $-20^{\circ}\text{C}$  for as long as 41 months did not cause an increase in aged CCP. Similarly, storage of the enzyme had no detectable effect on the electronic absorption spectrum or on the reaction of the native enzyme with hydrogen peroxide [12]. Instead, many of the differences reported in the literature are attributable to specific-ion effects, handling of the protein, and lyophilization.

In order to investigate the effect of source and experimental conditions on the coordination state of CCP, magnetic circular dichroism (MCD) spectroscopy has been employed. This technique has been shown to be especially valuable in studying the structural and magnetic properties of iron porphyrin systems [13,14]. MCD spectroscopy has certain advantages in that it requires only  $10^{-6}$ – $10^{-4}$  M sample concentrations, and it is applicable to any oxidation or spin state of a heme system even at ambient temperatures. Thus,

MCD spectroscopy has been extensively utilized for studies of the active site structures of numerous heme proteins [14], and has been shown to be a powerful probe of spin state, oxidation state (ferrous, ferric, ferryl), and axial ligation in heme systems [15,16]. In addition, the technique is relatively insensitive to the non-coordination environment of the chromophore in question. Comparison of MCD spectra of structurally defined heme complexes, either in proteins or synthetic models, with different oxidation and ligation states with the parallel derivatives of a structurally undefined heme protein can often lead to the establishment of the axial ligands of the latter [13–17]. Surprisingly, this technique has not been employed in studies of CCP, except in the UV region (250–350 nm) to study tryptophan residues within the protein [18] and in a recent investigation of the high-valent intermediates, Compound I and Compound II [19]. Here, we use MCD spectroscopy to probe the electronic and, therefore indirectly, the physical structure of the heme active site of the ferric protein in the absence of exogenous ligands. A detailed comparison is given of the MCD and electronic absorption properties of ferric yeast CCP (YCCP), recombinant CCP (CCP(MKT)), and lyophilized YCCP with those of ferric myoglobin (Mb) and ferric horseradish peroxidase (HRP), two extensively studied proximal histidine-ligated heme proteins. Additionally, the X-ray crystal structure of a CCP(MKT) sample which spectroscopically resembles lyophilized YCCP has been solved to 2.0 Å resolution.

## 2. Experimental

### 2.1. Materials and preparation of samples

Yeast CCP (YCCP) and recombinant CCP(MKT), expressed in *E. coli*, were purified as previously described [20,21]. Horseradish peroxidase (Sigma, Type VI) and horse heart myoglobin (Sigma) were obtained commercially. Both the yeast and recombinant forms of CCP were stored as crystal suspensions in distilled water [20,21] at  $-70^{\circ}\text{C}$  until needed. Once thawed, the suspension was spun down, and the supernatant discarded. Some crystals of YCCP were dried by lyophilization and stored for 2–3 days at room temperature. Samples stored in this manner are designated ‘lyophilized’ YCCP in this study. CCP crystals were dissolved in potassium phosphate buffer at  $4^{\circ}\text{C}$  and pH 6.0 or 7.0, as indicated, and the alkaline forms were prepared in potassium phosphate solution at pH 9.7 at concentrations of 60–70  $\mu\text{M}$ . Sample concentration was determined based on  $\epsilon_{408}=98$  ( $\text{mM cm}^{-1}$ ) for YCCP and CCP(MKT) [11], and  $\epsilon_{555}=34$  ( $\text{mM cm}^{-1}$ ) for the pyridine hemochrome [22] of the lyophilized YCCP. Samples of HRP and Mb whose MCD spectra were recorded in this study were prepared as described elsewhere [23]. The MCD spectrum of cytochrome  $b_5$  used in this study has been published elsewhere [24].

## 2.2. Spectroscopic techniques

Electronic absorption spectra were recorded on a Cary 210 spectrophotometer interfaced to an IBM PC. MCD spectra were measured using a 0.2 or 1.0 cm cuvette at 1.41 T with a JASCO J500-A spectropolarimeter. This instrument was equipped with a JASCO MCD-1B electromagnet and interfaced with a Gateway 2000 4DX2-66V PC through a JASCO IF-500-2 interface unit. The sensitivity of the instrument was  $10 \text{ m}^\circ \text{ cm}^{-1}$  for all scans with the time constant and scan rate selected to optimize the signal-to-noise ratio. Both MCD and CD signals and their respective baselines were recorded for all samples. The published MCD spectrum consists of the MCD signal minus its baseline and the sample's baseline-subtracted CD signal. All spectral measurements were performed at either 4 or 24°C as indicated, with data acquisition and manipulation being described elsewhere [25]. The MCD data were smoothed using a 17-point cubic routine in two iterations. Electronic absorption spectra were recorded before and after the MCD measurements to verify sample integrity. The spectra of CCP presented here are overlaid with spectra of the ferric derivatives of Mb, HRP and cyt  $b_5$  that have been presented elsewhere [23,24,26], or recorded in this study.

## 2.3. Structure determination of late growth CCP

Late growth recombinant CCP(MKT) was prepared by extending the culture times during expression from *E. coli*. As shown below, carefully controlled culture times (10 h) and induction periods (3 h) afford enzyme preparations with minimal spectroscopic differences from YCCP. Extending the culture time to 42 h results in enzyme preparations that are consistent with lyophilized YCCP. Single crystals of late growth CCP(MKT) were grown from 25% 2-methyl-2,4-pentanediol by sitting drop vapor diffusion using conditions previously described [27,28]. X-ray diffraction data were collected at 15°C using Cu K $\alpha$  radiation from a Siemens SRA rotating anode X-ray generator and a Siemens area detector. Data were indexed, integrated, merged and scaled using the Xengen suite of programs [29]. A model derived from WT CCP(MKT) (1cca) was used as the starting model for positional and *B*-factor refinements using SHELXL97 [30].

## 3. Results and discussion

We have examined various samples of CCP in its ligand-free ferric form using electronic absorption and MCD spectroscopies at neutral and alkaline pH. The electronic absorption (Fig. 1) and MCD data (Fig. 2) of the various species of CCP are compared to the spectra of exogenous ligand-free ferric derivatives of Mb and HRP, both of which also have a proximal histidine ligand. Table 1 summarizes the electronic absorption and MCD spectral data of the ferric CCP complexes examined. Electronic absorption maxima

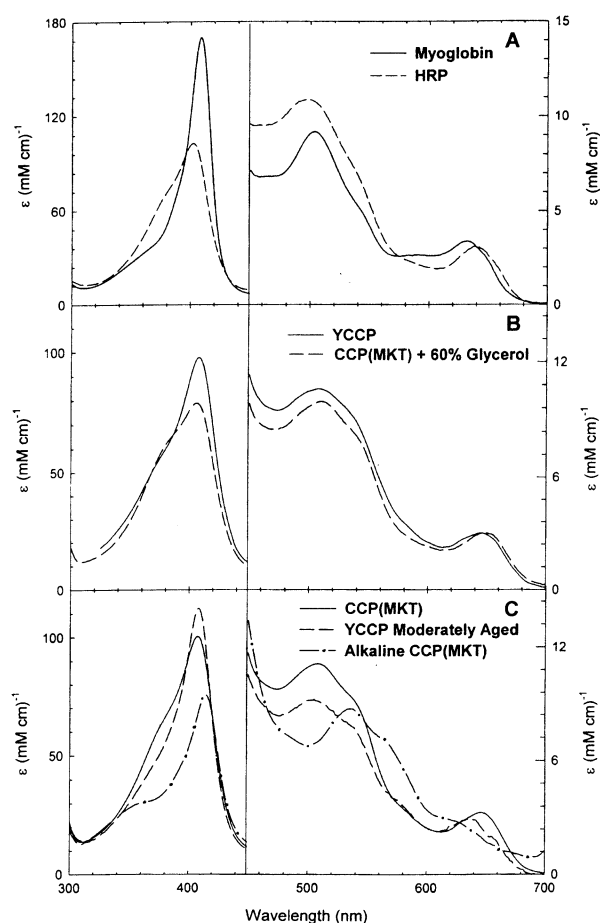


Fig. 1. Electronic absorption spectra (A) of the native ferric states of HRP in 0.5 M potassium phosphate buffer, pH 6.0 (dashed line), and Mb in 0.1 M potassium phosphate buffer, pH 7.0 (solid line), (B) the ferric states of YCCP in 0.05 M potassium phosphate buffer, pH 7.0 (solid line), and CCP(MKT) in 60% (v/v) glycerol 0.05 M potassium phosphate buffer, pH 7.0 (dashed line), (C) the ferric states of CCP(MKT) in 0.1 M potassium phosphate, pH 6.0 (solid line), lyophilized YCCP in 0.1 M potassium phosphate, pH 6.0 (dashed line), and alkaline CCP(MKT) in 0.1 M potassium phosphate buffer, pH 9.7 (dash-dotted line). CCP spectra were obtained at 4°C, using 40–70  $\mu\text{M}$  protein concentrations. The spectra for HRP and Mb are similar to those reported in [23,26].

and extinction coefficient values determined in this study are similar to those previously reported [11,23].

### 3.1. Coordination states of the heme iron of CCP at pH 7.0

The correlation between electronic absorbance and spin states of ferric hemoproteins has been well established [31–34]. Hexa-coordinate species such as ferric Mb (Fig. 1(A)) and its fluoride adduct exhibit narrow intense Soret absorption bands with extinction coefficients  $\geq 120 \text{ (mM cm)}^{-1}$  [12,34], whereas penta-coordinate high-spin heme proteins such as HRP (Fig. 1(A)) [35] and *Arthromyces ramosus* peroxidase [36] have a broader, more compressed Soret absorption band with extinction coefficients of about  $100 \text{ (mM cm)}^{-1}$ . The presence of a distinct shoulder in the 360–390 nm region, the noticeably intense CT band at 500–510

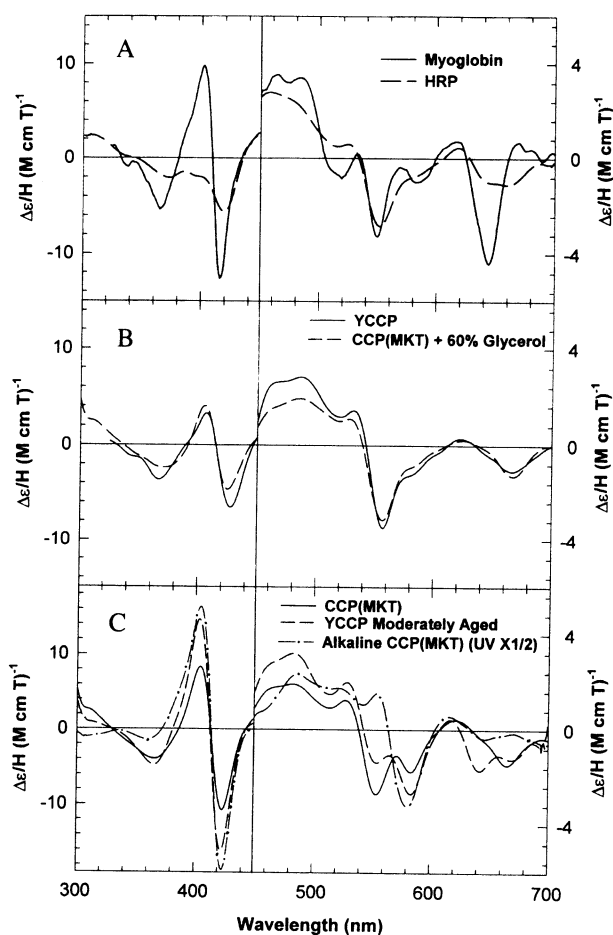


Fig. 2. MCD (A) of the native ferric states of HRP in 0.5 M potassium phosphate buffer, pH 6.0 (dashed line), and Mb in 0.1 M potassium phosphate buffer, pH 7.0 (solid line), (B) the ferric states of YCCP in 0.05 M potassium phosphate buffer, pH 7.0 (solid line), and CCP(MKT) in 60% (v/v) glycerol 0.05 M potassium phosphate buffer, pH 7.0 (dashed line), (C) the ferric states of CCP(MKT) in 0.1 M potassium phosphate, pH 6.0 (solid line), lyophilized YCCP in 0.1 M potassium phosphate, pH 6.0 (dashed line), and alkaline CCP(MKT) in 0.1 M potassium phosphate buffer, pH 9.7 (dash-dotted line, intensity divided by 2 in Soret region). CCP spectra were obtained at 4°C, using 40–70  $\mu$ M protein concentrations. The spectra for HRP and Mb are similar to those reported in [23,26].

nm, and a second red-shifted CT band ( $\sim 640$  nm) of low intensity are characteristic of the majority of penta-coordinated hydroperoxidases [35–37]. Vitello et al. [12] suggested that ratios of absorptivity of these wavelengths sensitive to the coordination and spin state of iron can be used to determine the presence of hexa-coordinate CCP in various CCP samples. Therefore, these ratios have been calculated for all CCP samples examined in this study and are listed in Table 2.

The electronic absorption spectrum of YCCP (pH 7.0) is shown in Fig. 1(B). The sample has a broad Soret peak at 408 nm with a distinct shoulder at  $\sim 370$  nm, similar to that of ferric HRP (penta-coordinate histidine-ligated, Fig. 1(A)). Additionally, a high-spin marker band can be seen at 645 nm which identifies the sample as fresh CCP [11,12]. This absorption spectrum yields values of 1.476 for the 408/

Table 1

Electronic absorption and MCD spectral features of different forms of CCP observed versus pH and aging

CCP forms	Absorption <sup>d</sup>		MCD	
	$\lambda$ max (nm)	$\epsilon$ ((mM cm) <sup>-1</sup> )	$\lambda$ (nm)	$\Delta\epsilon/H$ ((M cm T) <sup>-1</sup> )
YCCP <sup>a</sup> (pH 7.0)	408 <sup>d</sup>	98	390	0
			407	3.3
	507.5	106	415	0
			427	-6.6
	555 (sh)	6.5	487	2.8
CCP(MKT) <sup>b</sup> (pH 6.0)			531	1.4
	645	3.0	542	0
			557	-3.5
			667	-1.1
	408	100.4	404	8.36
CCP(MKT) in 60% glycerol (pH 6.0)			413	0
	507.5	11.2	423	-10.7
			481	1.9
	555 (sh)	6.7	527	1.25
			539	0
Lyophilized <sup>c</sup> YCCP (pH 6.0)	645.5	3.5	554	-2.7
			583	-1.8
			665	-1.5
	370 (sh)	56.3	391	0
	406	79	405	4.0
Alkaline CCP(MKT) (pH 9.7)			414	0
	509	9.9	425	-4.7
			486	1.9
	555 (sh)	6.0	528	1.1
			539	0
YCCP treated as outlined in Section 2.1.			557	-3.1
	649.5	3.0	667	-1.3
	408	112	403	14.7
			413	0
	501.5	9.2	423	-16.1
Similar $\lambda$ (and $\epsilon$ ) values have been previously reported for 'fresh' ferric YCCP [11].			483	3.2
	554 (sh)	5.7	529	2
			542	0
	637	3	554	-1.4
			584	-2.7
Fresh YCCP isolated from yeast [20].			642	-1.7
			669	-1.2
	360	36.5	401	41.4
			411	0
	414.5	86	421	-49.5
Recombinant wild-type CCP isolated from <i>E. Coli</i> [21,22].			482	1.6
	535	9.3	550	0.7
			557	0
	566 (sh)	6.8	579	-4.7
			610	0
YCCP treated as outlined in Section 2.1.	620	2.6	670	1.3

<sup>a</sup> YCCP: fresh CCP isolated from yeast [20].

<sup>b</sup> CCP(MKT): recombinant wild-type CCP isolated from *E. Coli* [21,22].

<sup>c</sup> YCCP treated as outlined in Section 2.1.

<sup>d</sup> Similar  $\lambda$  (and  $\epsilon$ ) values have been previously reported for 'fresh' ferric YCCP [11].

380 nm ratio and 0.7001 for the 620/647 nm ratio. Compared to the values determined by Vitello et al. (1.51 and 0.73) [12], the YCCP sample examined in this study appears to have a slightly lower percentage of hexa-coordinate character.

Table 2  
Ratio of absorptivities at conformationally sensitive wavelengths (nm) for ferric ligand-free CCP under varying conditions

CCP form	Ratio of absorptivities		MCD	
	UV-Vis		585 <sup>c</sup> /557 <sup>d</sup>	Soret peak-to-trough
	408/380 <sup>a</sup>	620/647 <sup>b</sup>		
YCCP, pH 7.0, 4°C <sup>e</sup>	1.48	0.70	0.3	9.9
CCP(MKT), pH 6.0, 4°C <sup>f</sup>	1.52	0.73	0.7	19.1
CCP(MKT), pH 6.0, 24°C <sup>f</sup>	1.51	0.71	0.4	17.5
CCP(MKT) + 60% glycerol pH 6.0, 4°C	1.27	0.71	0.3	8.7
Lyophilized YCCP pH 6.0, 4°C <sup>g</sup>	2.05	1.05	2.0	30.8
Lyophilized YCCP pH 6.0, 24°C <sup>g</sup>	1.96	1.02	1.0	20.9

<sup>a</sup> The maxima absorptivities occurred at 408 ± 1 nm.

<sup>b</sup> The maxima absorptivities occurred at 647 ± 3 nm.

<sup>c</sup> The maxima negative absorptivities occurred at 585 ± 2 nm.

<sup>d</sup> The maxima negative absorptivities occurred at 557 ± 2 nm.

<sup>e</sup> YCCP: fresh CCP isolated from yeast [20].

<sup>f</sup> CCP(MKT): recombinant wild-type CCP isolated from *E. coli* [21,22].

<sup>g</sup> YCCP treated as outlined in Section 2.1.

The MCD spectra of ferric YCCP can be seen in Fig. 2(B). In the visible region (450–700 nm), a single trough centered at ~555 nm is the dominant feature. This feature is also seen in the MCD spectrum of the prototypical peroxidase HRP (Fig. 2(A)). However, in the Soret region (300–450 nm) YCCP exhibits a low-intensity derivative-shaped transition that differs from the negative feature seen for HRP. Utilizing resonance Raman spectroscopy, Hildebrandt et al. [38] determined that, while YCCP at pH 7.0 is predominantly penta-coordinate, band fitting analysis of the relatively strong  $\nu_3$  mode at 1492 cm<sup>-1</sup> clearly reveals two minor components at 1485.1 and 1503.1 cm<sup>-1</sup>. These bands were assigned to hexa-coordinate high-spin (~7%) and hexa-coordinate low-spin (~9%) species, respectively. The MCD spectrum of YCCP thus represents a ferric heme that is predominantly high-spin, penta-coordinate, but possesses some hexa-coordinate high- and low-spin character [38]. Therefore, the derivative-shaped feature seen in the Soret region of the MCD spectrum is due to this hexa-coordinate character and can also be used to determine the presence of hexa-coordinate CCP in the sample. Accordingly, the distance from the peak to the trough of this feature has been included in Table 2 and will be used as a comparison for other CCP samples.

The electronic absorption and MCD spectra of ferric CCP(MKT) can be seen in Figs. 1(C) and 2(C), respectively. Similar to that of YCCP, the spectrum of CCP(MKT) shows a compressed Soret band at 408 nm with a distinct shoulder at about 370 nm. The visible region is also similar for the two proteins including the position of the CT band of CCP(MKT) at 645 nm, indicating comparable coordination structures for the two proteins. However, an analysis of the ratios of absorptivities at 408/380 and 620/647 nm (Table 2) between YCCP (1.476 and 0.7001) and CCP(MKT) (1.524 and 0.7264) indicates that the latter sample has a

somewhat higher percentage of hexa-coordinate form present.

Examination of the MCD spectra of CCP(MKT) (Fig. 2(B)) provides further support for the presence of a higher level of hexa-coordinate CCP in the sample. The Soret region reveals a slightly stronger derivative-shaped feature for CCP(MKT) (Fig. 2(B)) with a peak-to-trough distance of 19.1 compared to 9.9 for YCCP (Table 2). Furthermore, analysis of the visible region reveals that an additional trough at 583 nm is present only in the MCD spectrum of CCP(MKT). The trough at 583 nm is similar to that seen for various low-spin hexa-coordinate species such as alkaline HRP (a histidine/hydroxyl ligated heme) [39–42] and ferric Mb (Fig. 2(A)), allowing for its identification as a low-spin marker band for histidine-ligated ferric heme proteins.

In order to substantiate the presence of increased amounts of hexa-coordinate species in CCP(MKT), the electronic absorption has been examined in the presence of glycerol and at a higher temperature of 24°C. Both the addition of glycerol and the increase in experimental temperature have been shown to favor the penta-coordinate state of CCP [11,43,44]. The addition of 60% glycerol to CCP(MKT) yields a sample with spectroscopic characteristics more similar to YCCP than CCP(MKT) (Figs. 1(B) and 2(B), Table 1). The electronic absorption spectrum of CCP(MKT) in the presence of glycerol gives decreased ratios of 1.272 at 408/380 nm and of 0.7105 at 620/647 nm (Table 2). Similarly, in the MCD spectrum the peak-to-trough distance has decreased from 19.1 to 8.7, indicating that the addition of glycerol reduces the percentage of hexa-coordinate species in the CCP(MKT) sample. In particular, the loss of the MCD trough at 585 nm when glycerol is present confirms its identification as a hexa-coordinate low-spin marker band and indicates its potential

as an indicator of the presence of hexa-coordinate components in ferric CCP samples.

Similarly, an increase in temperature from 4 to 24°C results in a decrease in the amount of hexa-coordinate heme present in CCP(MKT). Both the electronic absorption and MCD data (data not shown) support this conclusion by yielding absorptivity ratios and a peak-to-trough distance that are lower at 24°C than at 4°C (Table 2). However, the effect of increasing the temperature on the presence of hexa-coordinate heme is not as drastic as the addition of glycerol to the sample. The decrease in hexa-coordinate species at higher temperatures is likely to be due to a destabilization of the water ligand located in the distal pocket, yielding a sample with a higher percentage of penta-coordinate character [43]. Thus, we conclude that CCP(MKT) is predominantly penta-coordinate high-spin with a slightly elevated amount of hexa-coordinate heme compared to YCCP.

With the identification of both ferric YCCP and CCP(MKT) as primarily penta-coordinate high-spin, we next attempted to determine the coordination environment of lyophilized ferric YCCP. The electronic absorption spectrum (Fig. 1(C), Table 1) shows that the Soret band at 408 nm has sharpened and intensified, while the CT band is blue-shifted to 637 nm. The location of the CT band at 637 nm indicates that the lyophilized YCCP has a lower percentage of hexa-coordination than samples investigated by Yonetani and Anni ( $\lambda_{CT} = 620$  nm) [11], but likely has a varied coordination from the CCP samples with a CT band at 645 nm. The ratios at 408/380 nm and 620/647 nm have both increased to 2.046 and 1.048 (Table 2), respectively, confirming the presence of increased amounts of hexa-coordinate species. In contrast, the trough at 554 nm is drastically reduced in intensity in the lyophilized YCCP spectrum compared to the 'fresh' YCCP spectrum, suggestive of a diminished amount of high-spin heme in the former.

Further support for this change in coordination structure can be seen in the MCD spectrum (Fig. 2(C)) of lyophilized YCCP. The derivative-shaped Soret feature in the MCD spectrum of the lyophilized YCCP sample has a peak-to-trough distance of 30.8, indicating a higher degree of low-spin hexa-coordination than in either YCCP or CCP(MKT). In addition, the intense trough at 584 nm yields a 585/557 nm ratio of 2.023, verifying a higher degree of low-spin character for lyophilized YCCP. An increase in temperature from 4 to 24°C results in a decrease in the amount of hexa-coordinate species in this sample as evidenced by decreases in the electronic absorptivity ratios of 408/380 and 620/647 nm, and in the MCD absorptivity ratio at 585/557 nm, and peak-to-trough distance of the derivative-shaped feature in the Soret region (Table 2). Again, this temperature dependence is likely to be due to the destabilization of the distal water ligand. Thus, the lyophilized sample of YCCP is predominantly a hexa-coordinate complex.

With the ability to identify the presence of hexa-coordinate CCP in our various CCP samples, it is of interest to determine methods useful in the removal of this coordination species.

Of the methods employed in this study, the addition of glycerol appears to be the best means of removing hexa-coordinate heme from the CCP samples (Table 2). Increasing the temperature to 24°C only partially converts hexa-coordinate to penta-coordinate heme (Table 2). It also appears that the extent of hexa-coordination of the CCP sample is a factor in the successful conversion to penta-coordinate species. Only the CCP(MKT) samples (~5% hexa-coordinate complex) could be fully transformed into the penta-coordinate form. For samples with a higher percentage of hexa-coordinate character, only a partial shift to the penta-coordinate state can be achieved. The level at which conversion to the hexa-coordinate species is permanent is presently unknown but is likely to be related to an irreversible conformational change due to conversion of the protein from penta- to hexa-coordination.

### 3.2. Identification of the distal ligand(s) in CCP(MKT) and lyophilized YCCP

In an attempt to reproduce the trough at 586 nm in the MCD spectrum of ferric CCP(MKT), mathematically merged MCD spectra have been constructed and compared to that of CCP(MKT) (data not shown). These model MCD spectra were composed of varying percentages and mixtures of metmyoglobin (a histidine/water ligated heme) [45], HRP–benzhydroxamic acid complex (a histidine/water ligated heme) [26], alkaline HRP (a histidine/hydroxide ligated heme) [39–42], and cytochrome  $b_5$  (a bis-histidine ligated heme) [46]. Analysis of these constructed MCD spectra demonstrated that only the merged spectrum containing 5% alkaline HRP and 95% YCCP has a trough at 586 nm [47]. The similarity between the merged MCD spectrum and that of CCP(MKT) indicates that the trough at 586 nm arises from low-spin, hexa-coordinate hydroxide-bound heme. This assignment is supported by the crystal structures of fresh YCCP [27] and CCP(MKT) [48] which show that Wat 595 is 2.6 Å from the heme and involved in three strong hydrogen bonds with Wat 596, Wat 648, and Trp 51. Due to these interactions and the distance from the heme iron, Wat 595 cannot be considered a strong ligand to the iron, which is consistent with the conclusion described above that CCP(MKT) is primarily penta-coordinate with only about 5% hexa-coordination in the form of histidine/hydroxide bound heme.

In an effort to determine the identity of the ligand complexes responsible for the MCD spectra of lyophilized ferric YCCP, the merged spectrum seen in Fig. 3(A) was constructed. Initially, the spectrum of 'fresh' YCCP was blended with those of the ferric HRP–benzhydroxamic acid complex (a histidine/water ligated heme) [26] and alkaline ferric HRP. Analysis indicates that the Soret region can be reasonably well duplicated, but the visible region cannot with the closest merged spectrum exhibiting two troughs with equal intensity (data not shown). The addition of 10% hexa-coordinate low-spin character in the form of ferric cytochrome  $b_5$  (bis-histidine ligated heme) [46] at the expense of the penta-

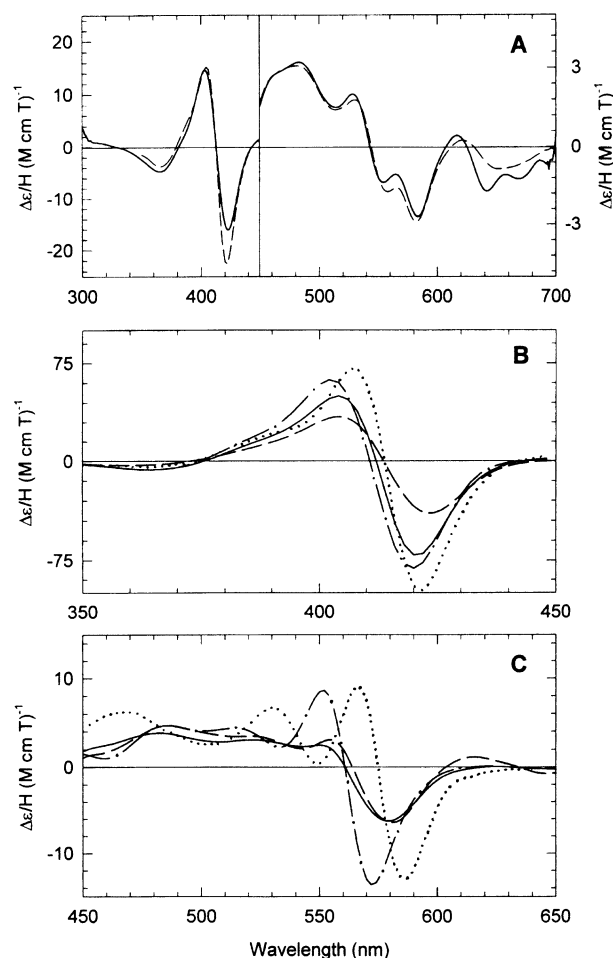


Fig. 3. MCD spectra (A) of the native ferric state of lyophilized YCCP in 0.1 M potassium phosphate buffer, pH 6.0 (solid line), and the merged spectrum (dashed line) consisting of 60% ferric YCCP, pH 7.0, 20% HRP–benzhydroxamic acid complex in 0.1 M potassium phosphate buffer, pH 7.0, 10% alkaline ferric HRP in 0.1 M potassium phosphate buffer, pH 12.0, and 10% ferric cytochrome  $b_5$  in 0.1 M potassium phosphate buffer, pH 7.0. MCD spectra (B and C) of alkaline ferric CCP(MKT) in 0.1 M potassium phosphate buffer, pH 9.7 (dashed line, intensity multiplied by 2 in (C)), alkaline ferric HRP in 0.1 M potassium phosphate buffer, pH 12.0 (dotted line), ferric cytochrome  $b_5$  in 0.1 M potassium phosphate buffer, pH 7.0 (dot-dashed line), and merged spectrum (solid line) consisting of 40% ferric YCCP, pH 7.0, 20% alkaline ferric HRP, pH 12.0 and 40% ferric cytochrome  $b_5$ , pH 7.0. The MCD spectra of alkaline HRP and cytochrome  $b_5$  are very similar to those previously reported [24,26].

coordinate high-spin YCCP species decreased the trough at 554 nm. The resulting merged MCD spectrum, which consisted of 60% YCCP, 20% HRP–benzhydroxamic acid complex, 10% alkaline HRP, and 10% ferric cytochrome  $b_5$ , simulates that of lyophilized YCCP very well (Fig. 3(A)) in band shape, position and intensity. This match indicates that lyophilized YCCP exists in a mixed-ligand state with water, hydroxide, and imidazole all serving as axial ligands. Attempts to exchange the MCD data of the ferric HRP–benzhydroxamic acid complex with that of ferric myoglobin were unsuccessful (data not shown). This inability to substitute ferric myoglobin into the model MCD spectrum is likely to be due to the variation of both the distal pocket ligand inter-

actions and the anionic character of the proximal ligand of CCP versus Mb. The requirement for a percentage of distal imidazole ligation in the merged spectrum substantiates the hypothesis that YCCP undergoes a conformational change under various conditions, which involves alteration of the disposition of the distal residues, bringing the distal His 52 into direct contact with ferric heme iron [49].

### 3.3. Identification of the distal ligand(s) in alkaline CCP(MKT)

Many ferric heme proteins undergo an alkaline transition from a high-spin form at neutral pH to a low-spin form at alkaline pH [50]. Resonance Raman studies have determined that the alkaline form of HRP contains a heme iron-ligated hydroxyl group [41] that is likely to form a hydrogen bond with a nearby protonated arginine residue (Arg 38) and the distal histidine (His 42) [42]. Due to the similarity of the distal pocket residues of HRP and CCP, the MCD spectrum of alkaline ferric CCP(MKT) has been compared to that of alkaline ferric HRP (Fig. 3(B) and (C)). The derivative shape of the spectrum of alkaline CCP(MKT) in both the visible and the Soret regions is less intense than those of alkaline HRP with the derivative-shaped feature in the visible region being about 20 nm blue-shifted as well. The basis for these discrepancies is likely to rest in the effect of increasing pH on the active-site pocket conformation of CCP. Studies by Smulevich et al. [51] have revealed that the replacement of distal His 52 with leucine in H52L CCP significantly modifies the nature of the transition from high- to low-spin under alkaline conditions. This implicates His 52 as a distal strong-field ligand in alkaline ferric CCP.

With the potential for His 52 ligation in the alkaline state of CCP, we compared the MCD spectrum of alkaline CCP(MKT) with that of ferric cytochrome  $b_5$  [46,52] (Fig. 3(B) and (C)). While the lineshapes are similar, the features of the spectrum of cytochrome  $b_5$  are all red-shifted and more intense than those of alkaline CCP(MKT). On closer inspection, the spectrum of alkaline CCP(MKT) appears to fall between that of cytochrome  $b_5$  and alkaline HRP in both feature intensity and position. Hence, a merged MCD spectrum consisting of 35% ferric alkaline HRP and 65% ferric cytochrome  $b_5$  was constructed which matched that of alkaline CCP(MKT) in lineshape and positioning, but not in intensity (Fig. 3(B) and (C)). The low intensity of the MCD spectrum of alkaline CCP(MKT) is likely to be due to the instability of CCP under alkaline conditions, as reported by Erman and co-workers [53–55]. Therefore, we suggest that a mixture of bis-histidine ferric heme and hydroxide/histidine-ligated ferric heme best represents the axial ligation of alkaline ferric CCP(MKT).

### 3.4. Effect of ferric heme iron coordination on the position of the electronic absorption CT band

Based on the findings described above, Fig. 4 schematically illustrates various ferric CCP forms which are com-

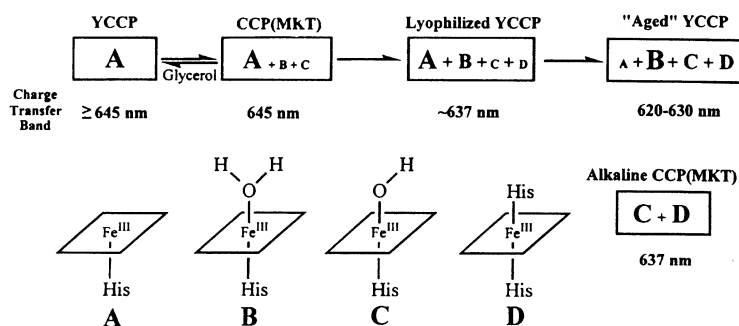


Fig. 4. Schematic depicting the coordination states of the varying forms of ferric CCP examined here and the position of their respective CT bands. The size of the letters reflects the relative contribution of the species A, B, C, and D to each CCP.

prised of two to four species in varying ratios. The CCP forms exhibit their CT bands between 645 and 620 nm depending on pH and degree of hexa-coordination. The CT band centered between 600 and 650 nm is due to CT between porphyrin and iron, and is sensitive to the  $\sigma$  and/or  $\pi$  donor capability of the axial ligands [56]. The lack of a sixth axial ligand results in a CT band around 643 nm as seen for ferric HRP [57], ferric cytochrome *c'* [57], and here for ferric YCCP. A transition to hexa-coordination appears to be accompanied by a blue shift in the CT band, as seen in cyanogen bromide-modified Mb versus ferric Mb (643 to 633 nm) [58], and in ferric HRP versus the benzhydroxamic acid complex of HRP (640 to 637 nm) [26]. The magnitude of the shift is dependent on the nature of the sixth ligand and the degree of hydrogen bonding between the axial ligands and the protein environment.

### 3.5. X-ray structural analysis of late growth CCP(MKT)

The spectroscopic data presented here demonstrate that YCCP (lyophilized YCCP) and recombinant CCP(MKT) (to a lesser degree) are sensitive to sampling handling-induced coordination state shifts. While MCD is a sensitive monitor of this alteration, and allows proposals for mixed His/hydroxy and bis-His species, the exact nature of the structural changes accompanying this coordination change is an important and unresolved issue. We have solved the room temperature crystal structure at 2.0 Å (Table 3) for a preparation of CCP(MKT) which was cultured for 42 h and exhibited the spectroscopic signatures of hexa-coordinate CCP. Examination of the electron density maps of Fig. 5 shows that the distal water molecule at 2.6 Å from the heme iron of penta-coordinate CCP(MKT) is either missing or moves closer to the iron in the late growth form of the enzyme, where it is observed only as an unresolved bulge of the intense iron density. Given that multiple lines of spectroscopic evidence have shown this form of the enzyme to be hexa-coordinate, the structure of late growth CCP(MKT) is interpreted as containing a closely bound water-derived ligand, fully consistent with the proposed His/hydroxy coordination. In addition, the N $\epsilon$  nitrogen of His-52 is observed to move slightly (0.5 Å) away from the heme in late growth

Table 3

X-ray diffraction data collection and refinement statistics for late growth CCP(MKT)

Data collection	
Unit cell <i>a</i> , <i>b</i> , <i>c</i> (Å)	104.2, 74.0, 45.5
Resolution (Å)	2.0
<i>I</i> / $\sigma$ <sub><i>i</i></sub> (av)	11.4
<i>I</i> / $\sigma$ <sub><i>i</i></sub> (last shell)	0.96
No. of reflections	22266
Completeness (%)	85
<i>R</i> <sub>sym</sub>	0.091
Refinement	
<i>R</i> <sub>cryst</sub>	0.185
Resolution (Å)	2.0
No. of reflections	19697
No. of waters	110

<sup>a</sup> Data were collected at 15 °C on a Siemens 3 axis area detector using Cu K $\alpha$  radiation and processed using Xgen [29]. The model was built using XtalView software [30] and refined in Shelxl97 [31]. *R*<sub>sym</sub> represents the agreement between *F*<sub>o</sub> for equivalent reflections. Values of *I*/ $\sigma$ <sub>*i*</sub>(last shell) represent the average *I*/ $\sigma$ <sub>*i*</sub> for the 10% of the data of highest resolution. The *R*<sub>cryst</sub> value is the crystallographic residuals for the observed and model-derived structure factor amplitudes for data with *F*<sub>o</sub> > 4 $\sigma$ <sub>*F*</sub>.

CCP(MKT) relative to the penta-coordinate enzyme, but no evidence exists for His-52 coordination to the heme. Despite this clear indication of a coordination state change at the heme, no other significant differences are observed in the protein structure between penta- and hexa-coordinate CCP(MKT). The rms difference for all heavy atoms between the structures of penta- and hexa-coordinate CCP(MKT) is only 0.21 Å. In addition, electrospray mass spectral analysis of penta- and hexa-coordinate CCP(MKT) yields identical masses to within 2 amu [59]. Possibly, deamidation of an asparagine or glutamine residue could result in the observed coordination-state changes without resulting in significant differences in the X-ray structure or mass of the protein. For example, His 52 makes a hydrogen bonding interaction with Asn 82, and the conversion of the latter to Asp could result in the observed spectroscopic changes.

We have examined the possibility that the small differences observed by MCD between YCCP and CCP(MKT) may



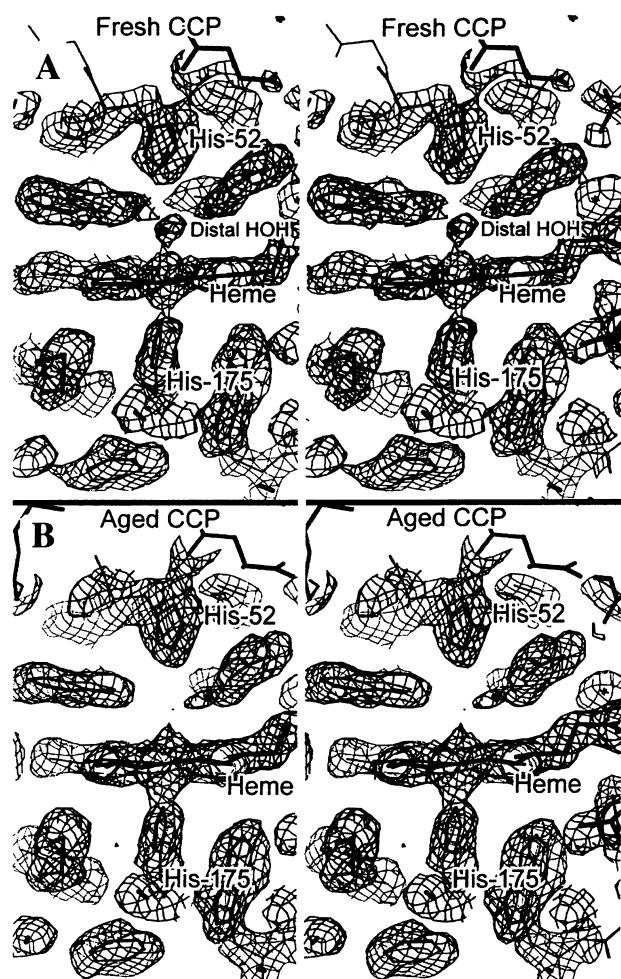


Fig. 5. Stereoviews of the refined crystal structures of (A) fresh CCP(MKT) (pdb entry 1cca) [48] and (B) aged CCP(MKT) superimposed on the  $2F_o - F_c$  electron density map contoured at  $1\sigma$ .

result from sequence variation. As has been noted previously [60,61], the sequence of CCP obtained from the laboratory strain of yeast (containing Ile-53 and Gly-152) used to clone the gene differs from that isolated from bakers yeast (containing Thr-53 and Asp-152). Reversion of these mutations was shown not to significantly affect the activity profile for the enzyme [60], but the subtle effects on spectroscopic signatures seen here may result from these differences. Comparison of published crystal structures for Bakers yeast CCP (2cyp) [62], penta-coordinate cloned CCP(MI) (1ccp) [27], penta-coordinate cloned CCP(MKT) (1cca) [48] and late growth CCP(MKT) (this work) show that the various structures are essentially identical near residue 53. Significant differences between these structures of approximately  $1\text{ \AA}$  are observed for residues more distant from the heme, including residue 152. However, these changes do not correlate with the identity of residue 152 and may result from packing effects in the different crystal forms, or in the slightly different N termini of the various forms. These proposals are able to be tested by mutagenesis studies currently under way.

## Acknowledgements

We thank Mark P. Roach for helpful discussions, Sheri Wilcox for cytochrome *c* peroxidase purification, and Drs Edmund Svastits and John J. Rux for assembling the MCD software. We also thank the reviewers of this manuscript for their helpful comments. Support was provided by NIH Grant GM 26730 (J.H.D) and GM 41049 (D.B.G.), and NSERC (Canada) (A.M.E.).

## References

- [1] H.R. Bosshard, H. Anni, T. Yonetani, in: J. Everse, K.E. Everse, M.B. Grisham (Eds.), *Peroxidases in Chemistry and Biology*, vol. II, CRC Press, Boca Raton, FL, 1991, p. 51.
- [2] T.L. Poulos, J.L. Kraut, *J. Biol. Chem.* 255 (1980) 8199.
- [3] B.C. Finzel, T.L. Poulos, J. Kraut, *J. Biol. Chem.* 259 (1984) 13027.
- [4] D.B. Goodin, A.G. Mauk, M. Smith, *Proc. Natl. Acad. Sci. USA* 83 (1986) 1295.
- [5] L.A. Fishel, J.E. Villafranca, J.M. Mauro, J. Kraut, *Biochemistry* 26 (1987) 351.
- [6] T. Yonetani, G.S. Ray, *J. Biol. Chem.* 240 (1965) 4503.
- [7] C.E. Nelson, E.V. Sitzman, C.H. Kang, E. Margoliash, *Anal. Biochem.* 83 (1977) 622.
- [8] A.M. English, M. Laberge, M. Walsh, *Inorg. Chim. Acta* 123 (1986) 113.
- [9] S. Dasgupta, D.L. Rousseau, H. Anni, T. Yonetani, *J. Biol. Chem.* 264 (1989) 654.
- [10] G. Smulevich, R. Evangelista-Kirkup, A.M. English, T.G. Spiro, *Biochemistry* 25 (1986) 4426.
- [11] T. Yonetani, H. Anni, *J. Biol. Chem.* 262 (1987) 9547.
- [12] L.B. Vitello, M. Huang, J.E. Erman, *Biochemistry* 29 (1990) 4283.
- [13] J.H. Dawson, M. Sono, *Chem. Rev.* 87 (1987) 1255.
- [14] J.H. Dawson, D.M. Dooley, in: A.B.P. Lever, H.B. Gray (Eds.), *Iron Porphyrins*, part III, VCH, New York, 1989, pp. 1–135.
- [15] L.E. Vickery, T. Nozawa, K. Sauer, *J. Am. Chem. Soc.* 98 (1976) 3.
- [16] S. Suzuki, T. Yoshimura, A. Nakahara, H. Iwasaka, S. Shidara, T. Matsubara, *Inorg. Chem.* 26 (1987) 1006.
- [17] E.J. Rigby, G.R. Moore, J.C. Gray, P.M.A. Gadsby, S.J. George, A.J. Thomson, *Biochem. J.* 256 (1988) 571.
- [18] D. Myers, G. Palmer, *J. Biol. Chem.* 260 (1985) 3887.
- [19] A.E. Pond, G.S. Bruce, A.M. English, M. Sono, J.H. Dawson, *Inorg. Chim. Acta* 275–276 (1998) 250.
- [20] A.M. English, M. Laberge, M. Walsh, *Inorg. Chim. Acta* 123 (1986) 113.
- [21] D.B. Goodin, M.G. Davidson, J.A. Roe, A.G. Mauk, M. Smith, *Biochemistry* 30 (1991) 4953.
- [22] K.G. Paul, H. Theorell, A. Akeson, *Acta Chem. Scand.* 7 (1953) 1284.
- [23] J.H. Dawson, S. Kadkhodayan, C. Zhuang, M. Sono, *J. Inorg. Biochem.* 45 (1992) 179.
- [24] E.W. Svastis, J.H. Dawson, *Inorg. Chim. Acta* 123 (1986) 83.
- [25] A.M. Huff, C.K. Chang, D.K. Cooper, K.M. Smith, J.H. Dawson, *Inorg. Chem.* 32 (1993) 1460.
- [26] A.M. Bracete, M. Sono, J.H. Dawson, *Biochim. Biophys. Acta* 1080 (1991) 264.
- [27] J.M. Wang, M. Mauro, S.L. Edwards, S.J. Oatley, L.A. Fishel, V.A. Ashford, N.H. Xuong, J. Kraut, *Biochemistry* 29 (1990) 7160.
- [28] M.M. Fitzgerald, M.J. Churchill, D.E. McRee, D.B. Goodin, *Biochemistry* 33 (1994) 3807.
- [29] A.J. Howard, C. Nielson, N.H. Xuong, *Methods Enzymol.* 114 (1985) 452.
- [30] G.M. Sheldrick, *Methods Enzymol.* 276 (1997) 628.
- [31] J. Beetstone, P. George, *Biochemistry* 3 (1964) 707.

- [32] D.W. Smith, R.J.P. Williams, *Biochem. J.* 110 (1986) 297.
- [33] T. Iizuka, T. Yonetani, *Adv. Biophys.* 1 (1970) 155.
- [34] W.A. Eaton, R.M. Hochstrasser, *J. Chem. Phys.* 49 (1968) 985.
- [35] R.A. Matthews, J.B. Wittenberg, *J. Biol. Chem.* 254 (1979) 5991.
- [36] N. Kunishima, F. Amada, K. Fukuyama, M. Kawamoto, T. Matsunaga, H. Matsubara, *FEBS Lett.* 378 (1996) 291.
- [37] S. Suzuki, T. Yoshimura, T. Sakurai, *J. Inorg. Biochem.* 44 (1991) 267.
- [38] P. Hildebrandt, A.M. English, G. Smulevich, *Biochemistry* 31 (1992) 2384.
- [39] T. Nozawa, N. Kobayashi, M. Hatano, *Biochim. Biophys. Acta* 427 (1976) 652.
- [40] M. Ikeda-Saito, H. Hori, L.A. Andersson, R.C. Prince, I.J. Pickering, G.N. George, C. Sanders II, R.S. Lutz, E.J. McKelvey, R. Mattera, *J. Biol. Chem.* 267 (1992) 22843.
- [41] A.J. Sitter, J.R. Shifflott, J. Turner, *J. Biol. Chem.* 263 (1988) 13032.
- [42] A. Feis, M.D. Marzocchi, M. Paoli, G. Smulevich, *Biochemistry* 33 (1994) 4577.
- [43] R. Evangelista-Kirkup, M. Crisanti, T.L. Poulos, T.G. Spiro, *FEBS Lett.* 190 (1985) 221.
- [44] G. Smulevich, A.R. Mantini, A.M. English, J.M. Mauro, *Biochemistry* 28 (1989) 5058.
- [45] S.V. Evans, D.G. Brayer, *J. Mol. Biol.* 213 (1990) 885.
- [46] G. Vergeres, L. Waskell, *Biochimie* 77 (1995) 604.
- [47] A.E. Pond, Ph.D. Dissertation, University of South Carolina, 1999.
- [48] D.B. Goodin, D.E. McRee, *Biochemistry* 32 (1993) 3313.
- [49] G. Smulevich, R. Evangelista-Kirkup, A.M. English, T.G. Spiro, *Biochemistry* 25 (1986) 4426.
- [50] E. Antonini, M. Brunori, in: *Hemoglobin and Mb and Their Reaction with Ligands*, North-Holland, Amsterdam, 1971, pp. 43–48.
- [51] G. Smulevich, M.A. Miller, J. Kraut, T.G. Spiro, *Biochemistry* 30 (1991) 9546.
- [52] I. Morishima, S. Ogawa, T. Inubushi, T. Iizuka, *Adv. Biophys.* 1 (1978) 217.
- [53] J.D. Satterlee, J.E. Erman, J.E. Mauro, J. Kraut, *Biochemistry* 29 (1990) 8797.
- [54] B.K. Dhaliwal, J.E. Erman, *Biochim. Biophys. Acta* 827 (1985) 174.
- [55] R.J. Dowe, J.E. Erman, *Biochim. Biophys. Acta* 827 (1985) 183.
- [56] G. Smulevich, F. Neri, M.P. Marzocchi, K.G. Welinder, *Biochemistry* 35 (1996) 10576.
- [57] L.B. Vitello, J.E. Erman, M.A. Miller, J.M. Mauro, J. Kraut, *Biochemistry* 31 (1992) 11524.
- [58] Y. Shiro, I. Morishima, *Biochemistry* 23 (1984) 4879.
- [59] D.B. Goodin, unpublished observations.
- [60] D.B. Goodin, M.G. Davidson, J.A. Roe, A.G. Mauk, M. Smith, *Biochemistry* 30 (1991) 4953.
- [61] J. Kaput, S. Goltz, G. Blobel, *J. Biol. Chem.* 257 (1982) 15054.
- [62] B.C. Finzel, T.L. Poulos, J. Kraut, *J. Biol. Chem.* 259 (1984) 13027.